

Macroinitiator Halide Effects in Galactoglucomannan-Mediated Single Electron Transfer-Living Radical Polymerization

Ulrica Edlund, Ann-Christine Albertsson

Fibre and Polymer Technology, School of Chemical Science and Engineering, Royal Institute of Technology (KTH), 100 44 Stockholm, Sweden

Correspondence to: A.-C. Albertsson (E-mail: aila@polymer.kth.se)

Received 23 June 2011; accepted 24 June 2011; published online 18 July 2011

DOI: 10.1002/pola.24855

ABSTRACT: Chloro (Cl)- and bromo (Br)-functionalized macroinitiators were successfully prepared from the softwood hemicellulose *O*-acetylated galactoglucomannan (AcGGM) and then explored and evaluated with respect to their ability and efficiency of initiating single electron transfer-living radical polymerization (SET-LRP). Both halogenated species effectively initiate SET-LRP of an acrylate and a methacrylate monomer, respectively, yielding brushlike AcGGM graft copolymers, where the molecular weights are accurately controlled via the monomer:macroinitiator ratio and polymerization time over a broad range: from oligomeric to ultrahigh. The nature of the halogen does not influence the kinetics of polymerization

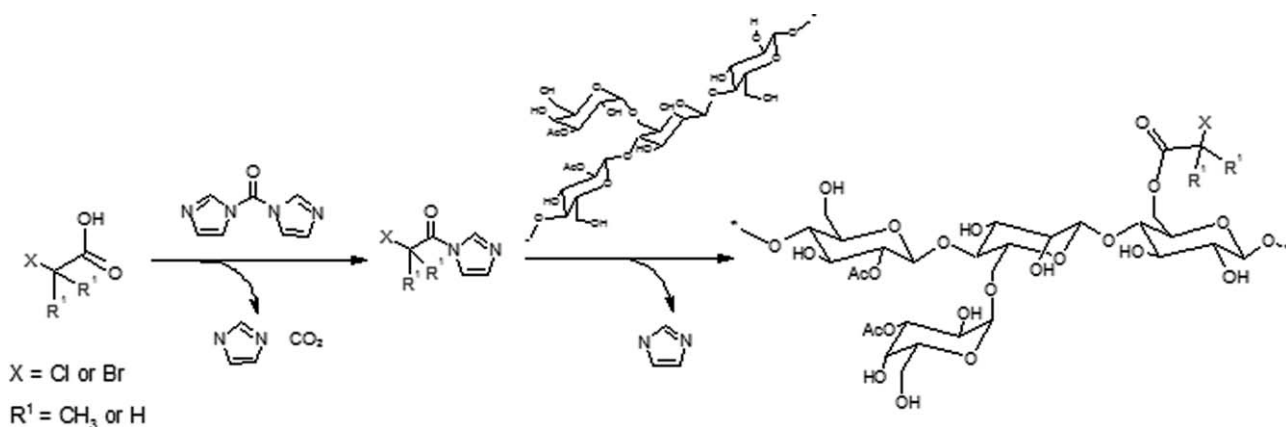
strongly, however, for acrylate graft polymerization, AcGGM-Cl gives a somewhat higher rate constant of propagation, while methacrylate grafting proceeds slightly faster when the initiating species is AcGGM-Br. For both monomers, the macroinitiator efficiency is superior in the case of AcGGM-Br. © 2011 Wiley Periodicals, Inc. *J Polym Sci Part A: Polym Chem* 49: 4139–4145, 2011

KEYWORDS: graft copolymers; hemicellulose; living polymerization; macroinitiator; polysaccharides; single electron transfer-living radical polymerization (SET-LRP); single electron transfer (SET)

INTRODUCTION The utilization of lignocellulosic feedstock through the conversion of its components into chemicals, materials, and energy is the core idea of the wood biorefinery concept. The recovery and purification of noncellulosic poly and oligosaccharides from such processes is possible via several pathways and opens up new opportunities for green material design. In recent years, hemicelluloses have attracted more and more attention as cheap and renewable resources, and we have elaborated pathways for various chemical modifications and the development of functional materials from the softwood hemicellulose *O*-acetylated galactoglucomannan (AcGGM).^{1–5} In a recent proof-of-concept study,⁶ this hemicellulose was successfully converted to a macroinitiator via an imidazole-driven activation of the sugar backbone pendant hydroxyl groups. The macroinitiator mediated the single electron transfer-living radical polymerization (SET-LRP) of a model vinyl monomer affording a hybrid graft glucopolymer with a brush-like architecture.

SET-LRP is a robust and versatile method for the living and controlled radical polymerization offering a fast pathway to well-defined vinyl polymers with a high level of control of the product structures, architectures, end groups, and molecular weights.^{7–10} In SET-LRP, the halide initiator induces reversibly terminated radical polymerization. The catalyst [typically a Cu(0) species] transfers a single electron to the

temporarily terminated macroradical, allowing for propagation until the catalyst/ligand complex generated in the process deactivates the propagating chain end back to a dormant state. The disproportionation of the catalyst/ligand complex in coordinating solvents such as water, alcohols, and other polar solvents is rapid and the driving force for a highly efficient polymerization.^{9,11} Compared with established living radical polymerization (LRP) techniques such as reversible addition-fragmentation-transfer¹² or atom transfer radical polymerization (ATRP),¹³ SET-LRP is robust toward oxygen,¹⁴ readily conducted in water containing media,¹¹ and offer facile removal of the metal catalyst.¹⁵ Simple monofunctional and difunctional initiators, such as the haloforms CHCl_3 and CHBr_3 , which are commonly used in LRP approaches, typically in ATRP but more recently also in SET-LRP. Also, alkyl halides and sulfonyl halides are viable and often used initiators. It has been shown that the nature of the halogen exerts only a minor effect on the polymerization, including the apparent rate constant of propagation (k_p^{app}) in SET-LRP,^{7,9} whereas in other metal-catalyzed LRP, typically ATRP, the k_{act} of the brominated initiator has been reported to be in the order of 10^3 – 10^4 greater than k_{act} of the corresponding chlorinated species.¹⁶ The outer sphere mechanism proposed for SET-LRP could explain this robustness of the SET-LRP process. Turning from small to macromolecular initiators presents new challenges but also a range of



SCHEME 1 Synthetic pathway for the preparation of AcGGM-based macroinitiators by 2-chloropropionic acid and α -bromo isobutyric acid. [Color figure can be viewed in the online issue, which is available at wileyonlinelibrary.com.]

opportunities. Various copolymer architectures are possible and far greater molecular weights are possible, but the higher initial molecular weight will affect the solubility and the reaction mixture viscosity posing potential limitations at higher conversions, successively decreasing the initiator efficiency over time, decelerating propagation and causing spontaneous precipitation before full conversion is reached. A multisite macroinitiator enable grafted and branched architectures with functional chain ends that allow for possible further coupling; however, small variations in site reactivity and accessibility might influence the kinetics and final structure and their viability for initiating polymerization in a living manner cannot be directly estimated from their low molecular weight analogs.

The aim of this work was to prepare chloro (Cl)- and bromo (Br)-substituted hemicellulose derived multisite macroinitiators for the grafting-from LRP and to provide a comparative assessment of the effect of the nature of the halogen in the SET-LRP of an acrylate and a methacrylate initiated from such glucomacroinitiators.

RESULTS AND DISCUSSION

Cl- and Br-functionalized macroinitiators were successfully prepared from the softwood hemicellulose AcGGM. These functionalized polysaccharides were then explored and evaluated with respect to their ability and efficiency of initiating the SET-LRP of two monomers, methyl acrylate (MA) and methyl methacrylate (MMA).

Both Cl- and Br-substituted hemicellulose-derived macroinitiators were prepared from the same type of hemicellulose backbone, a highly purified AcGGM. Bromination was performed using α -bromo isobutyric acid (α BrIBA) according to Scheme 1, whereas chlorination was afforded by 2-chloropropionic acid, yielding AcGGM-Br and AcGGM-Cl, respectively. The functionalization of AcGGM was structurally verified by ^1H NMR as shown in Figure 1. Neat AcGGM shows a characteristic cluster of overlaid peaks at 5.5–3.2 ppm stemming from the repeating unit anomeric hydrogens. The sharp peak at 2.16 ppm is assigned to the three protons in the ace-

tyl pendant groups. In the reaction with 2-chloropropionic acid, a methyl and a methine group is introduced, together with the $-\text{Cl}$ as a pendant moiety to the polysaccharide backbone, and these protons give rise to a set of nonresolved peaks ranging from 1.9 to 1.2 ppm in the ^1H NMR spectrum of AcGGM-Cl. The overlaid nature of these peaks is because of the substitution that may occur on several different carbons in the polysaccharide repeating unit. Substitution on C-6 is most likely due to steric effects and accordingly, one peak—at 1.69 ppm—is more pronounced than the others. For AcGGM-Br, $-\text{C}(\text{CH}_3)_2\text{-Br}$ moieties are introduced as pendant groups to the polysaccharide backbone giving rise to several methyl hydrogen peaks in the 2–1.1 ppm range.

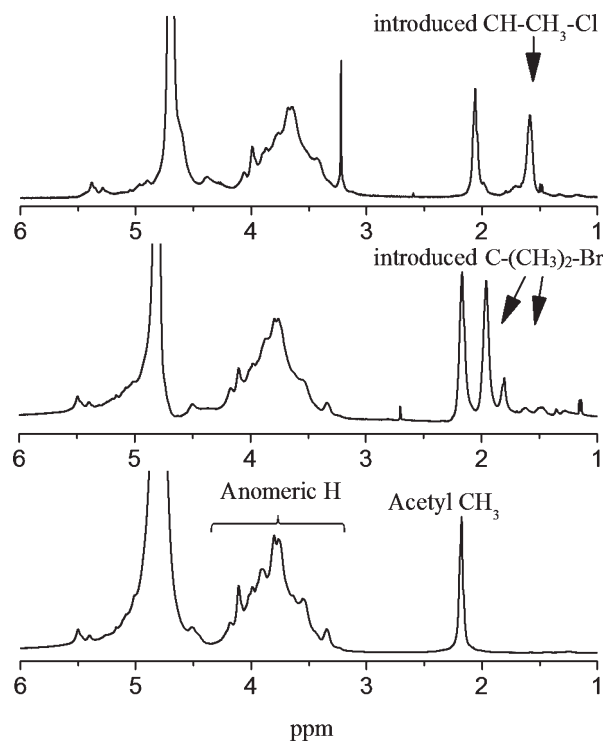
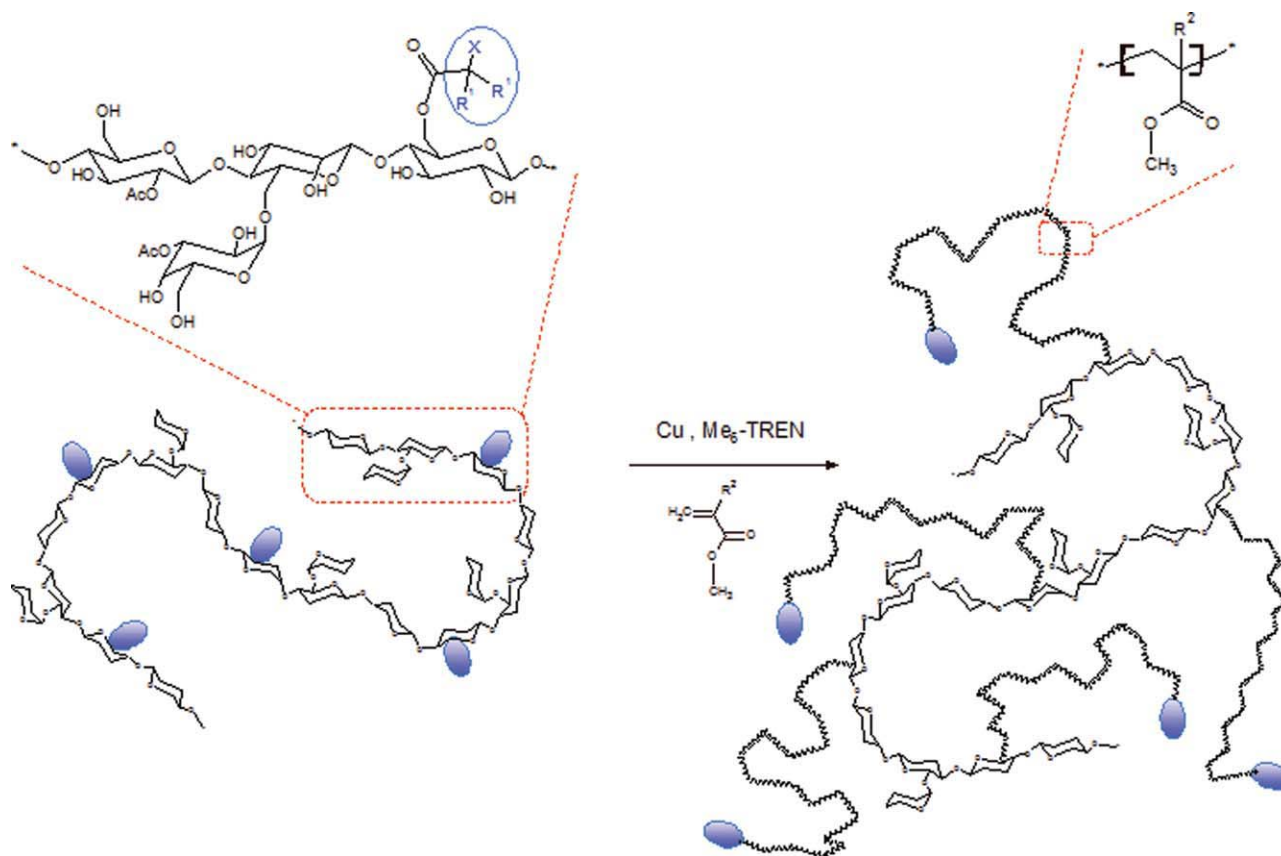


FIGURE 1 ^1H NMR in D_2O of native AcGGM (bottom), AcGGM-Br macroinitiator (middle), and AcGGM-Cl macroinitiator (top).



SCHEME 2 Synthetic pathway for the SET-LRP of MA and MMA using AcGGM-based macroinitiators. X is either Cl or Br, R¹ and R² denotes H or CH₃.

Again, some anomeric positions are preferred in the substitution reaction and accordingly, peaks at 1.96 and 1.80 ppm are the most pronounced.

The degree of acetylation (DS_{Ac}) in this particular hemicellulose sample is 0.3 as determined by size exclusion chromatography (SEC) calibrated with matrix assisted laser induced desorption and ionization - time of flight - mass spectrometry (MALDI-TOF-MS).^{17,18} Hence, the acetylation peak can be used as an internal standard in the calculation of the degree of substitution (DS) of Br- and Cl-substituents introduced to the hemicellulose backbone. Because of the more pronounced bulkiness of the α BriBA compared with 2-chloropropionic acid, the DS of the Br substituent (DS_{Br}) of functionalized AcGGM became somewhat lower than the corresponding DS_{Cl} , although the reaction time was doubled in the former case. DS_{Br} was 0.2, while DS_{Cl} was 0.3. The neat AcGGM had a M_w of 7500 g mol⁻¹ and the chlorinated AcGGM (AcGGM-Cl) had a M_w of 6630 g mol⁻¹, so there is a slight hydrolysis occurring at reaction times around 30 min at 50 °C. Brominated AcGGM (AcGGM-Br), on the other hand, had a M_w of 3450 g mol⁻¹ indicating that the longer reaction time, 1 h, caused a more significant hydrolysis of the AcGGM polysaccharide backbone. This difference in initiator molecular weight and degree of halogen substitution will affect the molecular weight of resulting graft copolymers that is possible to achieve during LRP at a fixed monomer:initiator ratio.

The halogenated AcGGMs were subsequently used in the SET-LRP of MA and MMA to elaborate their potential as macroinitiators. The resulting products are graft copolymers as schematically illustrated in Scheme 2. A model acrylate, MA, was polymerized by SET-LRP initiated by chlorine- and bromine-functionalized AcGGM, respectively, under identical reaction conditions. Kinetic plots are shown in Figures 2 and 3, respectively. The time dependence of $\ln [M_0]/[M]$ as well as the relationship between number-average molecular weight and conversion is close to linear in both cases suggesting a first-order rate of propagation and a living polymerization. The molecular weight distributions are not broadening over the course of polymerization but remains steadily around the values associated with the polysaccharide macroinitiators before grafting: 3.5 for AcGGM-Cl and 4.6 for AcGGM-Br, respectively, further sustaining this conclusion. Monomodal SEC traces are observed throughout the polymerizations. The initiator and monomer concentrations were purposely kept low to avoid very high viscosities with increasing conversions, yet the formation of a high viscosity reaction mixture was observed at high conversions, making it very difficult to reach full conversions. AcGGM-Br-initiated MA grafting proceeded at an apparent rate constant of propagation (k_{app}) of 0.0031 min⁻¹, while AcGGM-Cl-initiated MA grafting under identical conditions differed only to a minor extent with a k_{app} of 0.0035 min⁻¹. Compared with the SET-LRP of MA with a low molecular weight initiator analog,

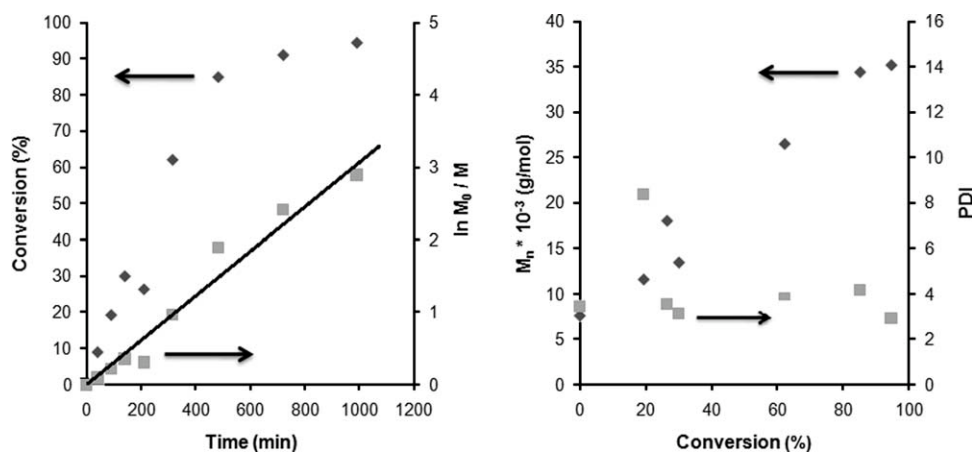


FIGURE 2 Kinetic plots for SET-LRP of MA initiated by AcGGM-Br. Each data point represents an individual experiment. Reaction conditions: $[MA]_0/[Cl\text{-}AcGGM]_0/[Me_6\text{-}TREN]_0 = 200/1/0.2$, 6.25 cm Cu-wire, DMSO = 3 mL, $[MA]_0 = 0.83 \text{ mol L}^{-1}$, 25 °C.

methyl 2-bromopropionate, under otherwise very similar conditions⁷ [dimethyl sulfoxide (DMSO), 25 °C, Cu(0), $[M]_0/[I]_0/[L]_0 = 2220/10/1$], the rate constants are a factor 16 lower for the AcGGM-macroinitiated SET-LRP of MA illustrating the change in initiator site accessibility when increasing the molar mass significantly. The ratio $k_{app}(\text{AcGGM-Cl})/k_{app}(\text{AcGGM-Br})$ is 1.13, which is sufficiently close to 1, to conclude that the nature of the halogen does not exert a strong influence on the propagation rate of MA when these AcGGM-derived multisite macroinitiators are used, in line with the outer sphere mechanism proposed for SET-LRP. However, it should be noted that the $k_{app}(\text{AcGGM-Cl})$ is slightly higher than $k_{app}(\text{AcGGM-Br})$ for the MA polymerization. The same trend was observed in the SET-LRP of MA initiated by haloforms, where $k_{app}(\text{CHCl}_3)/k_{app}(\text{CHBr}_3)$ was 1.25.⁷ In radical polymerization, the acrylates in general are expected to be more efficiently initiated by Br-initiators than Cl-initiators, whereas methacrylates, on the other hand, work better with Cl-initiators.¹⁰ This is not sustained by the results from AcGGM-initiated SET-LRP of MA, but the difference between the halide types is again not extensive as proposed for SET-LRP.⁷

MMA grafting-from AcGGM macroinitiators was typically more sluggish than MA grafting under the same conditions. Linear dependencies of $\ln [M]_0/[M]$ versus time and number-average molecular weight versus conversion still indicate a living behavior. Kinetic plots for MMA polymerization from AcGGM-Br and AcGGM-Cl are shown in Figures 4 and 5, respectively. Compared with AcGGM-Br-initiated MA grafting ($k_{app} = 0.0031 \text{ min}^{-1}$) under identical conditions, k_{app} was significantly lower in the case of MMA grafting: 0.0011 min^{-1} . In the case of AcGGM-Cl-initiated MMA grafting, the rate was even slower with a calculated $k_{app} = 0.0006 \text{ min}^{-1}$. The slower propagation of MMA compared with MA is also seen in conventional radical polymerization and other living approaches and is explained by the lower intrinsic k_p of methacrylates. The ratio $k_{app}(\text{AcGGM-Cl})/k_{app}(\text{AcGGM-Br})$ is in this case 0.56 which, in analogy with the MA polymerization described above, is sufficiently close to 1 to conclude that the nature of the halogen does not exert a strong influence on the propagation rate. In contrast to the MA polymerization, however, the $k_{app}(\text{AcGGM-Cl})$ is slightly lower than $k_{app}(\text{AcGGM-Br})$ for the MMA polymerization. As outlined

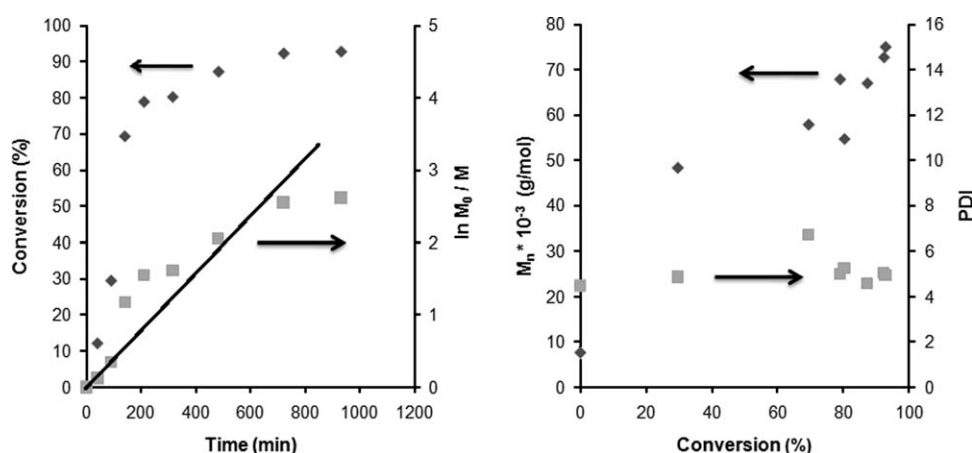


FIGURE 3 Kinetic plots for SET-LRP of MA initiated by AcGGM-Cl. Each data point represents an individual experiment. Reaction conditions: $[MA]_0/[Cl\text{-}AcGGM]_0/[Me_6\text{-}TREN]_0 = 2000/10/2$, 6.25 cm Cu-wire, DMSO = 3 mL, $[MA]_0 = 0.83 \text{ mol L}^{-1}$, 25 °C.

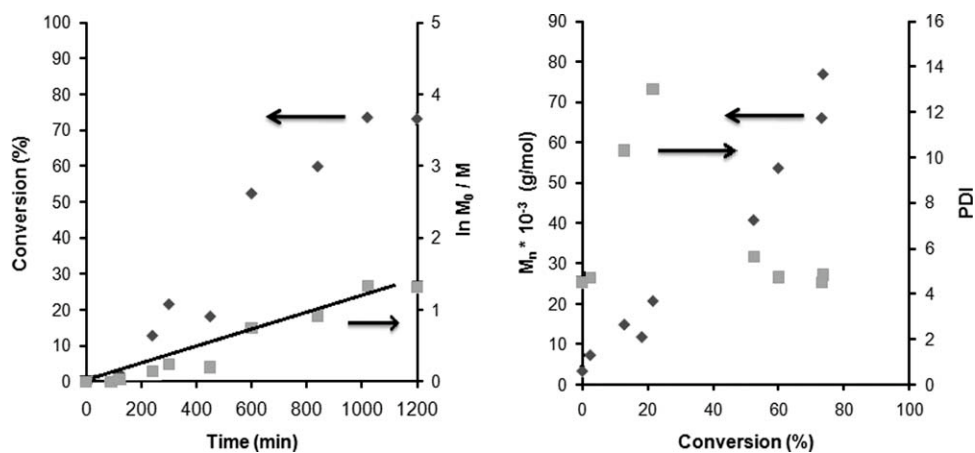


FIGURE 4 Kinetic plots for SET-LRP of MMA initiated by AcGGM-Br. Each data point represents an individual experiment. Reaction conditions: $[MMA]_0/[Cl\text{-}AcGGM]_0/[Me_6\text{-}TREN]_0 = 2000/10/2$, 6.25 cmCu-wire, DMSO = 3 mL, $[MMA]_0 = 0.83 \text{ mol L}^{-1}$, 25 °C.

previously, Cl-initiators are supposed to be better suited for the methacrylates than Br-initiators and vice versa for acrylates.¹⁰ As concluded for the AcGGM-initiated SET-LRP of MA in the previous paragraph, this relationship is not sustained by the results presented here. The halide affinities seems to be somewhat offset in the AcGGM-initiated SET-LRP, but still, the halide effects are small compared with those reported for other metal-catalyzed LRP.¹

In terms of product number-average molecular weight, there is a marked difference between polymerization initiated by the two AcGGM-based macroinitiators and a deeper perspective on their ability to function as macroinitiators is achieved by estimating the initiator efficiencies. When considering the products' number-average molecular weight as a function of the theoretical molecular weight as calculated according to the living polymerization theoretical dependence, a clear difference between the macroinitiators becomes apparent (Fig. 6). Initiator efficiencies, I_{eff} , of AcGGM-Cl range from 32 to 40%, whereas AcGGM-Br shows efficiencies in the range of 74–84%. The increase in I_{eff} for AcGGM-Br by a factor 2 coincides with the molecular weight of this macroinitiator

being only 50% of that of AcGGM-Cl. This means that much higher molecular weights are theoretically possible in the latter case but, at the same time, there is an increasing effect of steric hindrance in a random coil conformation of the longer chains potentially making initiator sites less available. Also, the viscosity buildup at higher conversions is more extensive hindering efficient diffusion and hence propagation. Clearly, the molar mass of the macroinitiator is a parameter significantly affecting the ability to effectively mediate SET-LRP and also a moderate increase in molar mass of the polysaccharide limit the initiator efficiency. Comparing I_{eff} values for the two monomers, respectively, sustain the small differences observed in halide suitability toward Cl- and Br-initiators. For the methacrylate, AcGGM-Br gave the higher k_{app} and also this initiator showed a higher I_{eff} for MMA ($I_{\text{eff}} = 84\%$) compared with MA ($I_{\text{eff}} = 74\%$) polymerization. For the acrylate, in contrast, AcGGM-Cl gave the higher k_{app} and, furthermore, the I_{eff} values for the Cl-initiator was higher for MA ($I_{\text{eff}} = 40\%$) than for MMA ($I_{\text{eff}} = 32\%$) polymerization. Hence, the I_{eff} values sustain the propagation rate trends, both trends contradicting the theoretic prediction that Cl-initiators are supposed to be better suited

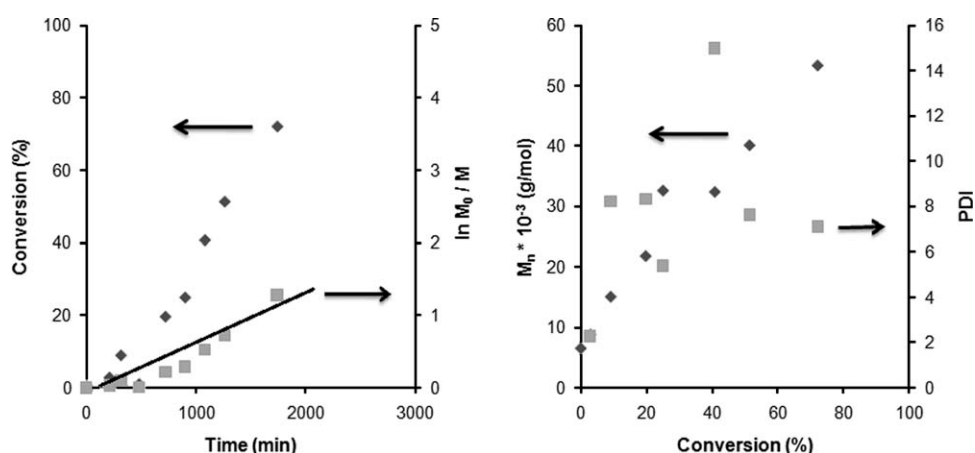


FIGURE 5 Kinetic plots for SET-LRP of MMA initiated by AcGGM-Cl. Each data point represents an individual experiment. Reaction conditions: $[MMA]_0/[Cl\text{-}AcGGM]_0/[Me_6\text{-}TREN]_0 = 2000/10/2$, 6.25 cm Cu-wire, DMSO = 3 mL, $[MMA]_0 = 0.83 \text{ mol L}^{-1}$, 25 °C.

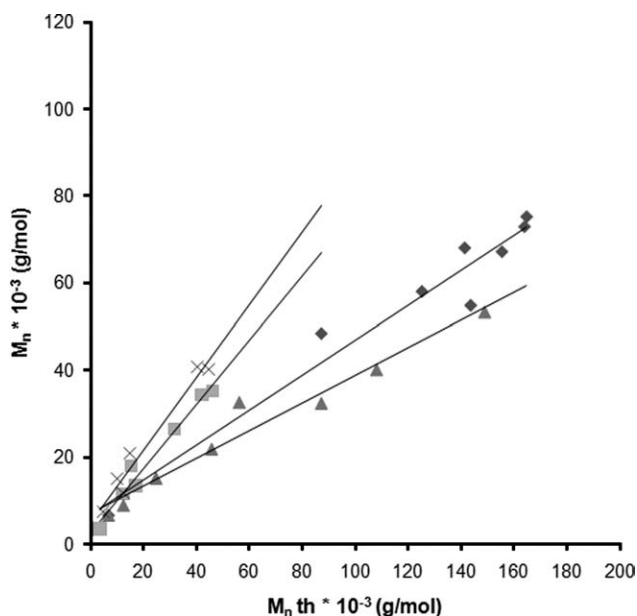


FIGURE 6 Molecular weights as measured by SEC versus theoretical molecular weights for macroinitiated SET-LRP: (x) MMA initiated by AcGGM-Br, (■) MA initiated by AcGGM-Br, (◆) MA initiated by AcGGM-Cl, and (▲) MMA initiated by AcGGM-Cl. Each data point represents an individual experiment. Reaction conditions: $[M]/[I]_0/[Me_6\text{-TREN}]_0 = 2000/10/2$, 6.25 cm Cu-wire, DMSO = 3 mL, 25 °C.

for the methacrylates than Br-initiators and vice versa for acrylates.¹⁰

To further elaborate the efficiency of Cl- and Br-AcGGM macroinitiators to mediate a polymerization in a living manner, the preparation of very high molecular weight polymers was attempted. Both types of AcGGM macroinitiators were, thus, used in the SET-LRP of MMA and MA with a $[M]_0/[I]$ ratio of 6000/1, catalyzed by Cu(0) and in DMSO at 25 °C as for the other experiments. Even though conducted at much lower concentrations to avoid a very high viscosity buildup, the reaction mixtures became close to solid, and higher conversions were not achieved. After 48 h, conversions up to 40% were reached. Still, very high and in a couple of experiments, ultrahigh, molecular weights were achieved. Similar I_{eff} values as calculated for the $[M]_0/[I] = 200/1$ experiments are observed here, $I_{\text{eff}} = 31\%$ for AcGGM-Cl and $I_{\text{eff}} = 60\%$ for AcGGM-Br. AcGGM grafted with poly(methyl methacrylate) (PMMA) where $M_n = 540,000$ and $M_w = 1,141,000$ ($M_w/M_n = 2.1$) were obtained after 48 h.

EXPERIMENTAL

Materials

N,N'-Carbonyldiimidazole (CDI) 97% (Aldrich), 2-chloropropionic acid (CPA) 98% (Sigma), α BrIBA 98% (Aldrich), tris(2-aminoethyl)amine 96% (Aldrich), formic acid $\geq 96\%$ (Aldrich), formaldehyde_{aq} 37% (AlfaAesar), dichloromethane 99.8% (Fisher), sodium chloride 99.5% (Merck), 2-propanol $\geq 99\%$ (LabScan), methanol $\geq 99.8\%$ (LabScan), copper wire (Fisher), acetone (Fischer, purum), and dimethylaceta-

mid 99.8% (Fisher), were used as received. DMSO $\geq 99.5\%$ (Fluka), MMA $> 99\%$ (Merck), and MA 99% (Merck) were distilled at reduced pressure before use.

O-Acetyl-galactoglucomannan (AcGGM) was recovered from the process water of thermomechanical pulping of spruce (*Picea abies*). The hemicellulosic fraction was concentrated by ultrafiltration, further purified by diafiltration, and finally lyophilized to yield off-white powder. The AcGGM had a weight average molecular weight of about 7500 g mol⁻¹, and a polydispersity index (PDI) of ~ 1.3 . The DS_{Ac} of 0.30 as determined by SEC calibrated with MALDI-TOF-MS.^{17,18}

Me₆-TREN Synthesis

Me₆-TREN was synthesized from 25.5 mL of 98% formic acid, 25 mL of 37% formaldehyde, and 6.58 g of tris(2-aminoethyl)amine (0.045 mol, 1 equiv) in 25 mL of H₂O according to a literature procedure.¹⁹

Yield: 10%. ¹H NMR (DMSO-*d*₆): $\delta = 2.50$ ppm (tr, 6 H, CH₂); 2.26 ppm (tr, 6 H, CH₂); 2.12 ppm (s, 18 H, N-(CH₃)₂); ¹³C-NMR (DMSO-*d*₆): $\delta = 57.43, 52.52, 45.64$ ppm.

AcGGM-Cl Macroinitiator Synthesis

AcGGM was converted to a macroinitiator by esterification of the sugar hydroxyl groups. In the first step, 2.130 g of CPA (23.25 mmol) was activated through coupling to CDI (3.768 g/23.25 mmol) in 20 mL of DMSO at room temperature. After 1 h, the temperature was raised to 50 °C and 1.50 g of AcGGM (8.65) dissolved in 100 mL of DMSO was added to the mixture and allowed to react with the imidazolyl activated CPA for 30 min. The product was precipitated in ethyl acetate and washed repeatedly with ethyl acetate. The crude precipitate was collected by centrifugation and purified with Soxhlet extraction for 2 days. The product was finally dissolved in water, lyophilized, and characterized with ¹H NMR and SEC.

AcGGM-Br Macroinitiator Synthesis

AcGGM was brominated analogous to the above described chlorination route using α BrIBA. α BrIBA (10.02 g/60 mmol) was activated with equimolar amounts of CDI (9.73 g) in 80 mL DMSO at room temperature. After 1 h, the temperature was raised to 50 °C and 2.60 g of AcGGM dissolved in 100 mL of DMSO was added together with an additional 4.08 g of CDI. The reaction was allowed to proceed for 60 min and quenched by precipitation in 2-propanol. The crude product was collected by centrifugation and purified with Soxhlet extraction with 2-propanol for 2 days. The product was finally dissolved in water, lyophilized, and characterized with ¹H NMR and SEC.

Polymerizations

All polymerizations were conducted in DMSO using Me₆-TREN as the ligand, and MA or MMA as the monomer. In a typical polymerization, the monomer, macroinitiator (Br-AcGGM or Cl-AcGGM), and ligand were dissolved in DMSO in a 2000:10:2 molar ratio. For 3 mL of solvent, 16.35 mg of Br-AcGGM or 8.4 mg of Cl-AcGGM were used. The monomer, macroinitiator, and ligand solution was in each polymerization transferred to a dry Schlenk-tube and degassed with six

consecutive freeze-pump-thaw cycles, flushing with nitrogen after thawing. Copper wire (6.25 cm) with a diameter of ~ 0.812 mm corresponding to American wire gauge 20, was used as a catalyst. The wire was wrapped around the stirring bar and kept over the reaction mixture throughout the degassing. Then, the tube was immersed in a thermostated oil bath at 25 °C, and the polymerization was started by dropping the stirring bar with the copper catalyst into the solution. The polymerization was monitored via ^1H NMR and SEC. Each data point is derived from an individual experiment. When reaching the individual stop time for each experiment, an aliquot of the reaction mixture was first sampled for NMR analysis under a flow of N_2 (g) using a syringe. The polymerizations were then terminated by precipitation of the reaction mixture in cold methanol. The product graft copolymers were then purified by redissolution in DMSO and reprecipitation in methanol followed by centrifugation and vacuum drying. For polymerizations aiming at ultrahigh molecular weights, monomer:macroinitiator:ligand ratios of 60,000:10:2 were used. The amounts were reduced to one-fourth of the amounts used for all other polymerizations as described. Sampling, product recovery, and purification were done according to the procedure described above.

Characterization

Molecular weights were determined with a Shimadzu SEC system equipped with four PLgel 20 μm Mixed-A columns and using *N,N*-dimethylacetamide (DMAc) as the eluent with a flow rate of 0.5 mL min^{-1} at 80 °C and an injection volume of 200 μL . Pullulan standards with narrow molecular weight distributions were used for calibration. All samples were dissolved in DMAc containing LiCl (0.5%, w/w) and filtered before analysis.

^1H NMR spectra were recorded at 400 MHz on a Bruker DMX-400 nuclear magnetic resonance spectrometer with Bruker software. DMSO- d_6 and D_2O (Larodan Fine Chemicals AB) were used as solvents, and spectra were recorded in sample tubes with an outer diameter of 5 mm.

CONCLUSIONS

The hemicellulose AcGGM was successfully converted to Cl- and a Br-functionalized macroinitiators using an imidazole-mediated esterification of the pendant hydroxyl groups on the polysaccharide backbone. Both halogenated species effectively initiated SET-LRP of methyl acrylate (MA) and methyl methacrylate (MMA) in DMSO solution yielding grafted AcGGM copolymers. The Cl- and the Br-functionalized macroinitiators show small differences in rates of SET-LRP. For acrylate graft polymerization, AcGGM-Cl gives the highest apparent rate constant ($k_{\text{app}} = 0.0035 \text{ min}^{-1}$), while methacrylate grafting proceeds at a higher k_{app} (0.0011 min^{-1}), when the initiating species is AcGGM-Br. For both

monomers, the macroinitiator efficiency of AcGGM-Br is twice as high when compared with AcGGM-Cl, influenced by the higher initial chain length of the latter and the associated viscosity effects at high molecular weights of the hybrid graft copolymer products. The molar mass of the macroinitiator is a parameter significantly affecting the ability to effectively mediate SET-LRP, even a moderate increase in molar mass of the polysaccharide limit the initiator efficiency. Both Cl- and Br-functionalized AcGGM successfully mediate the formation of very high or ultrahigh molecular weight graft copolymers. Weight average molecular weights exceeding 1 million g mol^{-1} were achieved from AcGGM-Cl-initiated SET-LRP.

REFERENCES AND NOTES

- 1 Lindblad, M. S.; Ranucci, E.; Albertsson, A. C. *Macromol Rapid Commun* 2001, 22, 962–967.
- 2 Hartman, J.; Albertsson, A. C.; Sjöberg, J. *Biomacromolecules* 2006, 7, 1983–1989.
- 3 Edlund, U.; Albertsson, A. C. *J Bioact Compat Polym* 2008, 23, 171–186.
- 4 Voepel, J.; Edlund, U.; Albertsson, A. C. *J Polym Sci Part A: Polym Chem* 2009, 47, 3595–3606.
- 5 Edlund, U.; Ryberg, Y. Z.; Albertsson, A. C. *Biomacromolecules* 2010, 11, 2532–2538.
- 6 Voepel, J.; Edlund, U.; Albertsson, A. C.; Percec, V. *Biomacromolecules* 2011, 12, 253–259.
- 7 Percec, V.; Guliashvili, T.; Ladislaw, J. S.; Wistrand, A.; Stjern Dahl, A.; Sienkowska, M. J.; Monteiro, M. J.; Sahoo, S. *J Am Chem Soc* 2006, 128, 14156–14165.
- 8 Lligadas, G.; Percec, V. *J Polym Sci Part A: Polym Chem* 2008, 46, 2745–2754.
- 9 Lligadas, G.; Percec, V. *J Polym Sci Part A: Polym Chem* 2008, 46, 4917–4926.
- 10 Percec, V.; Rosen, B. M. *Chem Rev* 2009, 109, 5069–5119.
- 11 Percec, V.; Nguyen, N. H.; Rosen, B. M.; Jiang, X.; Fleischmann, S. *J Polym Sci Part A: Polym Chem* 2009, 47, 5577–5590.
- 12 Moad, G.; Rizzardo, E.; Thang, S. H. *Aust J Chem* 2005, 58, 379–410.
- 13 Matyjaszewski, K.; Xia, J. H. *Chem Rev* 2001, 101, 2921–2990.
- 14 Percec, V.; Jiang, X. A.; Rosen, B. M. *J Polym Sci Part A: Polym Chem* 2010, 48, 2716–2721.
- 15 Percec, V.; Nguyen, N. H.; Rosen, B. M.; Lligadas, G. *Macromolecules* 2009, 42, 2379–2386.
- 16 Matyjaszewski, K.; Paik, H. J.; Zhou, P.; Diamanti, S. J. *Macromolecules* 2001, 34, 5125–5131.
- 17 Jacobs, A.; Lundqvist, J.; Stalbrand, H.; Tjerneld, F.; Dahlman, O. *Carbohydr Res* 2002, 337, 711–717.
- 18 Dahlman, O.; Jacobs, A.; Liljenberg, A.; Olsson, A. I. *J Chromatogr A* 2000, 891, 157–174.
- 19 Ciampolini, M.; Nardi, N. *Inorg Chem* 1966, 5, 41–44.